Access of Quaternary Ammonium Blockers to the Internal Pore of Cyclic Nucleotide-gated Channels: Implications for the Location of the Gate

Jorge E. Contreras and Miguel Holmgren

Porter Neuroscience Research Center, National Institute of Neurological Disorders and Stroke, National Institutes of Health, Bethesda, MD 02892

Cyclic nucleotide-gated (CNG) channels play important roles in the transduction of visual and olfactory information by sensing changes in the intracellular concentration of cyclic nucleotides. We have investigated the interactions between intracellularly applied quaternary ammonium (QA) ions and the α subunit of rod cyclic nucleotide-gated channels. We have used a family of alkyl-triethylammonium derivatives in which the length of one chain is altered. These QA derivatives blocked the permeation pathway of CNG channels in a concentration- and voltage-dependent manner. For QA compounds with tails longer than six methylene groups, increasing the length of the chain resulted in higher apparent affinities of ~1.2 RT per methylene group added, which is consistent with the presence of a hydrophobic pocket within the intracellular mouth of the channel that serves as part of the receptor binding site. At the single channel level, decyltriethyl ammonium (C10-TEA) ions did not change the unitary conductance but they did reduce the apparent mean open time, suggesting that the blocker binds to open channels. We provide four lines of evidence suggesting that QA ions can also bind to closed channels: (1) the extent of C10-TEA blockade at subsaturating [cGMP] was larger than at saturating agonist concentration, (2) under saturating concentrations of cGMP, cIMP, or cAMP, blockade levels were inversely correlated with the maximal probability of opening achieved by each agonist, (3) in the closed state, MTS reagents of comparable sizes to QA ions were able to modify V391C in the inner vestibule of the channel, and (4) in the closed state, C10-TEA was able to slow the Cd^{2+} inhibition observed in V391C channels. These results are in stark contrast to the well-established QA blockade mechanism in Kv channels, where these compounds can only access the inner vestibule in the open state because the gate that opens and closes the channel is located cytoplasmically with respect to the binding site of QA ions. Therefore, in the context of Kv channels, our observations suggest that the regions involved in opening and closing the permeation pathways in these two types of channels are different.

The Journal of General Physiology

INTRODUCTION

Cyclic nucleotide-gated (CNG) channels are nonselective cation channels which mediate the transduction of visual and olfactory signals (Stryer, 1986, 1988; Yau and Baylor, 1989; Lagnado and Baylor, 1992; Zufall et al., 1994; Menini, 1995; Zimmerman, 1995). The activity of CNG channels accurately follows the changes in the intracellular concentration of cyclic nucleotide that occur in response to a stimulus. As a result, the chemical potential of intracellular cyclic nucleotide is converted into an electrical potential, driving subsequent steps in the visual and olfactory signal cascades (Stryer, 1986, 1988; Yau and Baylor, 1989; Lagnado and Baylor, 1992; Zufall et al., 1994; Menini, 1995; Zimmerman, 1995; Kaupp and Seifert, 2002).

CNG channels are tetramers formed by the coassembly of homologous subunits (Chen et al., 1993; Liu et al., 1996; Bonigk et al., 1999; Pages et al., 2000; Weitz et al., 2002; Zheng et al., 2002; Zhong et al., 2002; Peng et al., 2004; Zheng and Zagotta, 2004). CNG subunits contain six transmembrane segments similar to the subunits that form voltage-activated K^+, Na^+, and Ca^{2+} channels, which suggests that all these channels belong to the same superfamily (Jan and Jan, 1990). At present, there are four α (CNGA1, 2, 3, and 4) and two β (CNGB1 and 3) subunits that have been cloned from vertebrate organisms (Kaupp and Seifert, 2002). CNGA1, CNGA2, and CNGA3 can form functional homotetramers conferring most of the electrophysiological and pharmacological properties (Kaupp et al., 1989; Dhallan et al., 1990; Bonigk et al., 1993). Functional expression of β subunit homotetramers has not been observed. However, α and β subunits do coassemble (Chen et al., 1993; Bonigk et al., 1999; Pages et al., 2000), apparently with a 3α:1β stoichiometry in rod CNG channels (Weitz et al., 2002; Zheng et al., 2002; Zhong et al., 2002) while with a 2α:2β stoichiometry in cone CNG channels (Peng et al., 2004).

CNG channels are blocked or inhibited allosterically by a variety of molecules: divalent cations (Colamartino

Correspondence to Miguel Holmgren: holmgren@ninds.nih.gov

Abbreviations used in this paper: CNG, cyclic nucleotide-gated; QA, quarternary ammonium.

Volume 127 Number 5 May 2006 481–494
http://www.jgp.org/cgi/doi/10.1085/jgp.200509440

et al., 1991; Zimmerman and Baylor, 1992; Root and MacKinnon, 1993; Tanaka and Furman, 1993; Zufall and Firestein, 1993; Eismann et al., 1994; Root and MacKinnon, 1994; Picones and Korenbrot, 1995; Nasi and del Pilar Gomez, 1999; Seifert et al., 1999), tetraalkylammonium ions (Stotz and Haynes, 1996), L-cis-diltiazem (Quandt et al., 1991; Haynes, 1992; McLatchie and Matthews, 1992, 1994), tetracaine and its derivatives (Fodor et al., 1997a,b; Ghatpande et al., 2003; Strassmaier et al., 2005), inactivation ball peptide (Kramer et al., 1994), polyamines (Lu and Ding, 1999; Lynch, 1999), pseudechetoxin (Brown et al., 1999), diacylglycerol (Crary et al., 2000), retinoids and analogues (Dean et al., 2002; Horrigan et al., 2005), and dequalinium (Rosenbaum et al., 2003, 2004).

In potassium channels, the blockade mechanisms by quaternary ammonium (QA) ions have provided tremendous insights into the structure and function of this class of channels. In voltage-activated potassium (Kv) channels, intracellularly applied QA compounds block K^+ current by binding within the permeation pathway (Armstrong, 1971; Choi et al., 1993; Holmgren et al., 1997; del Camino et al., 2000). Under some circumstances, Kv channels can trap QA ions by closing the channel (Armstrong, 1971; Armstrong and Hille, 1972; Holmgren et al., 1997). These results suggest that there is a cavity within the K^+ permeation pathway that is large enough to accommodate a QA ion ($\sim$10 Å in diameter), and that the gate that opens and closes the pore in response to voltage is positioned below this cavity. This model was further supported by gated accessibility studies with MTS reagents (Liu et al., 1997) and by the crystal structure of KcsA channel in the presence of tetrabutylantimony (Zhou et al., 2001).

In CNG channels, our understanding on the gating mechanisms is less refined. Even though conformational changes associated with cGMP activation have been demonstrated in the P-region (Liu and Siegelbaum, 2000; Mazzolini et al., 2002) and the S6 transmembrane segment (Flynn and Zagotta, 2001), we do not have a clear picture of where the channel opens and closes in response to cGMP. Motivated by the fruitfulness of the use of QA blockade in clarifying the gating mechanism of Kv channels, we have embarked in a detailed characterization of the interactions between alkyl-triethylammonium derivatives and the inner mouth of CNGA1 channels. We found that some of the blockade properties of QA ions in CNG channels are similar to those observed in Kv channels. For example, QA derivatives bind within the permeation pathway, blockade is voltage dependent ($\delta \sim -0.4$), and blocker and channel interact predominantly through hydrophobic interactions. However, whereas in Kv channels QA compounds only bind to the pore after the activation gate opens, in CNG channels they can bind when the activation gate is either open or closed. These results provide further evidence that the gating mechanisms in CNG and Kv channels are distinct.

MATERIALS AND METHODS

DNA Expression

cDNA of the CNGA1 subunit from bovine rod photoreceptor (Kaupp et al., 1989) and the cysteine-less CNGA1 channel were provided by W. Zagotta (University of Washington, Seattle, WA). CNGA1 wild-type channel was subcloned in the GW1-CMV vector (British Biotechnology) for expression in HEK293 cells (American Type Culture Collection) as previously described (Holmgren, 2003). The cysteine-less CNGA1 channel did not express in mammalian cells, so experiments using this construct were performed with *Xenopus* oocytes as the expression system (Matulef et al., 1999). cRNA was synthesized using a T7 promoter-based in vitro synthesis (Ambion). Cysteine substitution at position 391 was confirmed by sequencing performed at the DNA Sequencing Facility in NINDS. cRNA was injected into *Xenopus* oocytes and recordings were performed 3–5 d after injection.

Solutions and Electrophysiological Recordings

The solutions contained (in mM) 160 (or 120 when using *Xenopus* oocytes) NaCl, 1 EGTA, 1 EDTA, 10 HEPES, pH 7.4 adjusted with NaOH. When Cd^{2+} ions were used, divalent chelators were removed from our recording solutions. Na salts (puriss, p.a. grades) were purchased from Fluka. Divalent chelators, cyclic nucleotides (Na salts), tetraethylammonium, hexyltriethylammonium, and $CdCl_2$ were obtained from Sigma-Aldrich, and HEPES was acquired from American Bioanalytical. MTS-PrtEA and MTSET were purchased from Toronto Research Chemical. Longer tail QA compounds and MTSTEA reagent were provided by G. Yellen (Harvard University, Boston, MA; Choi et al., 1993; Holmgren et al., 1996). Currents from inside-out excised patches (Hamill et al., 1981) were recorded using an Axopatch 200B amplifier (Axon Instruments Inc.). Records in the absence of cGMP were subtracted to isolate macroscopic cGMP-dependent currents. Macroscopic data analysis was performed with pClamp 9 (Axon Instruments Inc.) and Origin 7 (Microcal Software Inc.) software. Macroscopic currents were sampled at 2.5–10 kHz and low-pass filtered at 1 or 2 kHz. Patches with macroscopic currents were obtained with borosilicate glass pipettes between 2 and 3 MΩ. Single channel recordings were sampled at 20 kHz and filtered at 5 kHz with an 8-pole Bessel filter (Frequency Devices). Before analysis, single channel records were digitally filter at 2 kHz and analyzed with software provided by B. Rothberg (University of Texas Health Science Center, San Antonio, TX) and K. Magleby (University of Miami School of Medicine, Miami, FL). Pipettes between 7 and 10 MΩ were used in single channel experiments. Excised patches were physically positioned in close proximity to the inlet of the chamber. Solutions were switched manually or by a computer-controlled rapid solution changer (RSC-200, Biologic Science Instruments). To assure steady-state conditions, assessment of blockade was usually made 10–40 s after solution exchange. Upon blocker removal, cGMP-dependent currents recovered completely within 0.5–2 s.

RESULTS

Blockade of CNGA1 Channels by C10-TEA

The interactions between QA compounds and heterologous expressed bovine rod CNGA1 channels were

studied using inside-out patches excised from HEK293 cells. To isolate cGMP-dependent currents, records in the absence of cGMP were subtracted from those obtained in its presence. Fig. 1 A shows leak-subtracted currents acquired in response to voltage steps between −80 and +80 mV from a holding potential of 0 mV, and in the presence of a saturating concentration of cGMP. In the same inside-out patch, the effect of increasing concentrations of C10-TEA added to the bath solution is shown in Fig. 1 (B–F). The normalized dose response measured at the end of the pulse to +80 mV is shown in Fig. 2 A. The following Hill equation was fitted to the dose response data:

$$\frac{I_{C10\text{-}TEA}}{I} = \frac{1}{1+\left(\frac{[C10-TEA]}{K_D}\right)^n}, \quad (1)$$

where $I_{C10\text{-}TEA}$ is the current in the presence of blocker, I is the current without C10-TEA, K_D is the C10-TEA apparent affinity, [C10-TEA] is the concentration of C10-TEA applied to the bath and n is the Hill coefficient. The best-fit parameter values for K_D and n were 21.5 ± 0.6 μM and 1.19 ± 0.04, respectively. Because n is close to 1, we tentatively assume that, at +80 mV, one molecule of C10-TEA is sufficient to block the current through a CNG channel. A noticeable feature of the C10-TEA blockade mechanism in CNG channels is its voltage dependence, reflected as a time-dependent current decrease at positive potentials and a current increase at negative potentials (Fig. 1, B–F). We can estimate the apparent affinity at different voltages by the relation:

$$K_D = (I_f \times [C10\text{-}TEA]) / (1 - I_f), \quad (2)$$

where I_f is the fractional current remained after blockade. Fig. 2 B displays the voltage dependence of the apparent affinity for C10-TEA. The relatively simple relationship between these two variables allows us to fit a Woodhull-type voltage-dependent model to the values of K_D (Woodhull, 1973):

$$K_D(V) = K_D0 \times e^{z\delta FV/RT}, \quad (3)$$

where K_D0 is the value of K_D at 0 mV, z is the valence of the blocker (1 for C10-TEA), δ is the electrical distance, and R, T, and F have their usual meaning and values. The best-fit parameter values for K_D0 and δ were 72.0 ± 1.0 μM and −0.44 ± 0.01, respectively. From a total of 10 different patches, the average values for K_D0 and δ were 50 ± 10 μM and −0.47 ± 0.04, respectively.

A Hydrophobic Pocket for QA Derivatives

A molecule of C10-TEA can be viewed as formed by two regions, a hydrophilic positively charged head provided by the quaternary ammonium group and a relatively hydrophobic tail composed by a saturated carbon chain of 10 carbons (Fig. 3, top left). To establish which region of the C10-TEA molecule contributes most to the binding energy, we designed an experiment in which we assessed blockade by other QA derivatives with either a smaller head and the same tail or the same head but a smaller tail. Fig. 3 shows five consecutive leak-subtracted current traces acquired in the same inside-out patch in response to a voltage step from 0 to +80 mV. The first trace shows the cGMP-sensitive current under control

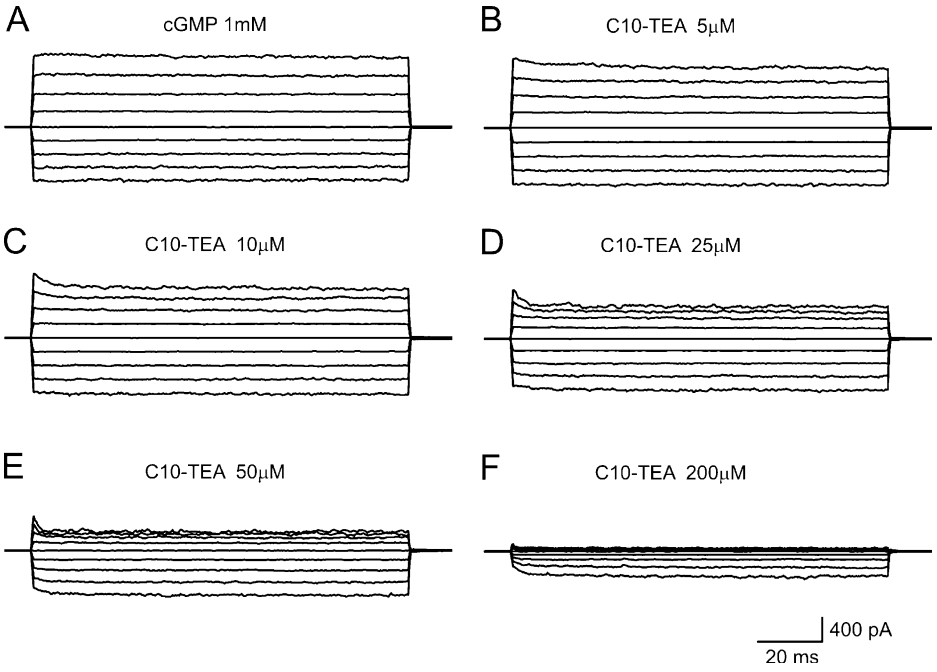

Figure 1. C10-TEA blocks CNG channels. Leak-subtracted currents in response to 1 mM cGMP in the absence (A) and in the presence (B–F) of increasing concentrations of C10-TEA. All these current traces were acquired from the same inside-out patch and in response to voltage jumps from −80 to +80 mV in steps of 20 mV, from a holding potential of 0 mV.

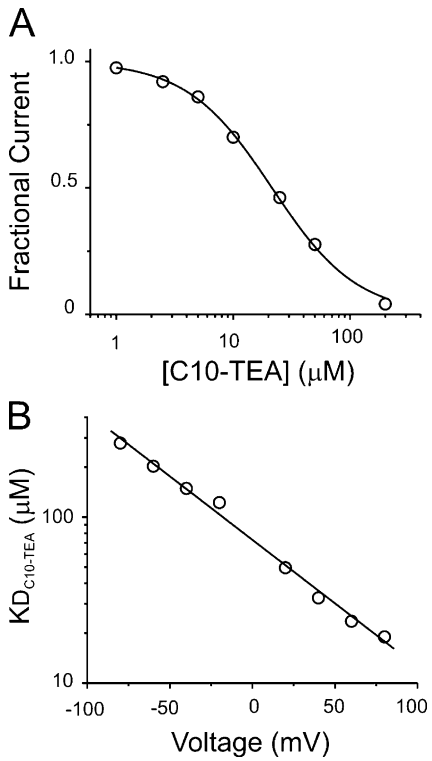

Figure 2. General properties of C10-TEA blockade. (A) Normalized dose–response at +80 mV. The solid line represents the fit to a Hill equation (see text; Eq. 1). The best-fit parameter values for K_D and n were 21.5 ± 0.6 μM and 1.19 ± 0.04, respectively. (B) Voltage dependence of C10-TEA blockade. K_D values at each voltage were estimated by Eq. 2. The solid line represents the fit to a Woodhull-type model (Eq. 3). The best-fit parameter value for δ is −0.45.

conditions (i.e., 1 mM cGMP in the absence of blocker). To set up the reference condition, we proceeded to evaluate blockade by 50 μM C10-TEA (Fig. 3, second trace from the left). Blockade levels by 50 μM decyl-trimethyl ammonium (smaller head, same tail) showed a mere 1.8-fold difference in apparent affinity as compared with blockade observed by C10-TEA (Fig.3, third trace). However, blockade by 100-fold higher concentration of TEA (same head, smaller tail) resulted in only ∼35% reduction in current (Fig. 3, fourth trace). Even though this experiment has not been designed to test the importance or necessity of the charged group of these compounds on blockade, it qualitatively shows that the tail of C10-TEA is likely to be a major contributor to the apparent binding affinity to CNGA1 channels.

To more quantitatively examine the contribution of the tail, we evaluated blockade by a series of QA derivatives with successively smaller hydrophobic chains. Fig. 4 shows an experiment where blockade by four QA compounds was assessed in the same inside-out patch. Blockade levels obtained by 50 μM C10-TEA could be achieved by QA derivatives with smaller chains only at much higher concentrations (0.5 mM C8-TEA, 10 mM C6-TEA, and 20 mM C4-TEA; Fig. 4 B), which suggests that the hydrophobic tail of these compounds plays an important role in determining the binding energy. The voltage dependence of blockade in this experiment is shown in Fig. 4 C. Solid lines represent Woodhull model fits to the data (see figure legend for best-fit parameter values). The average δ values for the different blockers were −0.31 ± 0.04 (TEA, $n = 4$), −0.40 ± 0.08 (C3-TEA, $n = 2$), −0.40 ± 0.03 (C4-TEA, $n = 7$), −0.48 ± 0.02 (C6-TEA, $n = 7$), −0.43 ± 0.02 (C8-TEA, $n = 10$), and −0.43 ± 0.02 (C10-TEA, $n = 10$). Except for TEA where the δ value seems to be slightly smaller, the voltage dependence of blockade by all QA derivatives is similar. A noticeable property for the smaller compounds, however, is the tendency at positive potentials to deviate from linearity (Fig. 4 C). This phenomenon could arise from either permeation of the blocker (traditional view) or by permeant ions tuning the voltage dependence of the blocker (Spassova and Lu, 1999). The average K_D0 values (μM) for the different blockers were 35,000 ± 4,000 (TEA, $n = 4$), 31,000 ± 4,000 (C3-TEA, $n = 2$), 11,000 ± 2,000 (C4-TEA, $n = 7$), 5,000 ± 1,000

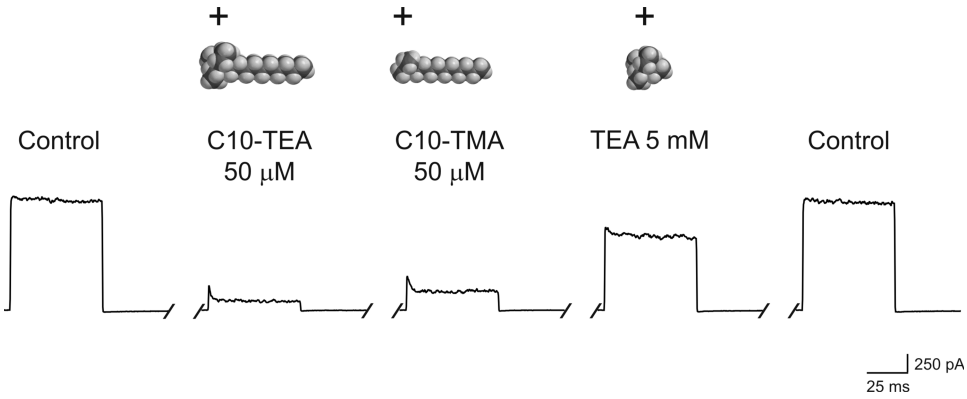

Figure 3. The tail of C10-TEA is a major contributor to the binding affinity to CNG channels. Leak-subtracted currents from five consecutive traces in the presence of 1 mM cGMP to a voltage step of +80 mV, from a holding potential of 0 mV. All traces were obtained from the same inside-out patch. The first trace from the left was acquired in the absence of any blocker, the second in the presence of 50 μM C10-TEA, the third with 50 μM C10-TMA, the fourth with 5 mM TEA, and finally the experiment was bracketed with control conditions. Between traces, the patch was perfused with a solution devoid of cGMP and blocker for at least 30 s. Leak currents were acquired during these periods and they showed no changes throughout the experiment.

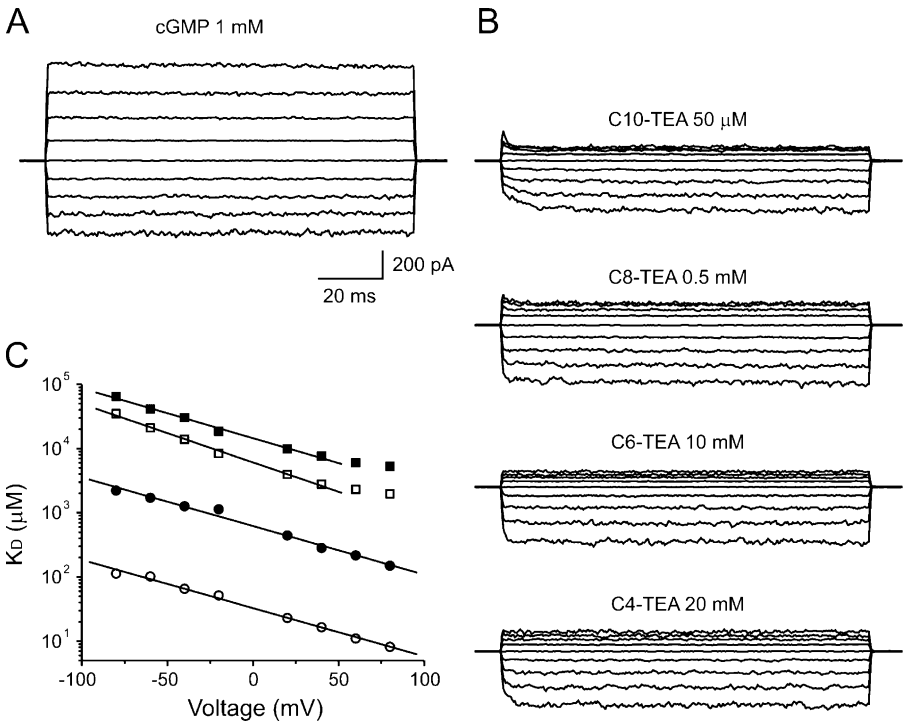

Figure 4. General properties of blockade by alkyl-TEA derivatives. (A) Control conditions. Leak-subtracted currents in the presence of 1 mM cGMP acquired in response to voltage jumps from −80 to +80 mV in steps of 20 mV, from a holding potential of 0 mV. (B) Leak subtraction currents from the same patch and under the same conditions as A, but in the presence of QA derivatives with successively smaller alkyl chains. (C) Voltage dependence of blockade by QA derivatives. K_D values at each voltage were estimated by Eq. 2. Solid lines represent Woodhull model fits (Eq. 3). The best-fit parameter values for δ and K_D were −0.44 ± 0.01, 32 ± 2 μM (C10-TEA; open circles); −0.44 ± 0.02, 605 ± 7 μM (C8-TEA; filled circles); −0.53 ± 0.02, 6144 ± 21 μM (C6-TEA; open squares); −0.45 ± 0.02, 14642 ± 35 μM (C4-TEA; filled squares).

(C6-TEA, $n = 7$), 900 ± 200 (C8-TEA, $n = 10$), and 50 ± 10 (C10-TEA, $n = 10$). By converting the K_D0s to apparent binding energies (ΔG) arbitrarily compared with a 1 M standard ($\Delta G = -RT \ln(1M/K_D0)$; Choi et al., 1993), we can estimate the binding energy contribution of each methylene group in the tail of the blocker (Fig. 5). The straight line represents a linear regression fit of the values of ΔG/RT for the longer QA derivatives, showing that the binding energy increases by 1.22 RT per methylene group added to the tail. This value is in good agreement with the energy needed to transfer a methylene group from a nonpolar medium to an aqueous solution (Tanford, 1980). As previously observed in Kv channels (Choi et al., 1993), shorter QA blockers deviate from the predicted hydrophobic interactions. Taken together, these results suggest that somewhere in the intracellular mouth of the channel there is a hydrophobic pocket that contributes to the binding site for QA compounds.

C10-TEA Binds within the Permeation Pathway

Even though the voltage dependence of C10-TEA (Figs. 1 and 2) is an indication that the blocker binds within the permeation pathway, the voltage dependence could also arise from blocker binding within a cavity in the protein along which there is a voltage drop, as it has been suggested for the voltage dependence of ion translocation during transport in ATPases (Gadsby et al., 1993). Traditionally, the effects of extracellular permeant ions on intracellular blockade have been used as evidence of blocker binding within the permeation pathway. Unfortunately, we were unable to use this strategy because we found that the traditional ion substitutes (e.g., NMDG, TMA, and amino acids) interact with the external mouth of CNG channels (unpublished data; Stotz and Haynes, 1996). Instead, we evaluated the effect of external Mg^{2+} on intracellular C10-TEA blockade. External divalent cations are thought to block and permeate through CNG channels by interacting with a glutamate residue in the P loop of CNG channels (Root

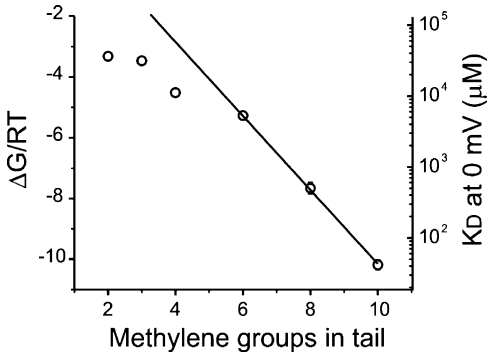

Figure 5. Binding energy decreases as the length of the alkyl tail is shortened. The binding energy of each blocker was calculated from the values of K_D0 by assuming an arbitrary standard concentration of 1 M ($\Delta G = -RT \ln(1M/K_D0)$). Binding energies are plotted in RT units. The line represents a fit of the binding energies for C6-, C8-, and C10-TEA to a straight line. The best-fit value for the slope is −1.22 ± 0.03, which means an increase of binding energy of ∼1.2 RT for each additional methylene group. Except for C8- and C10-TEA, all standard errors are smaller than the size of the symbols.

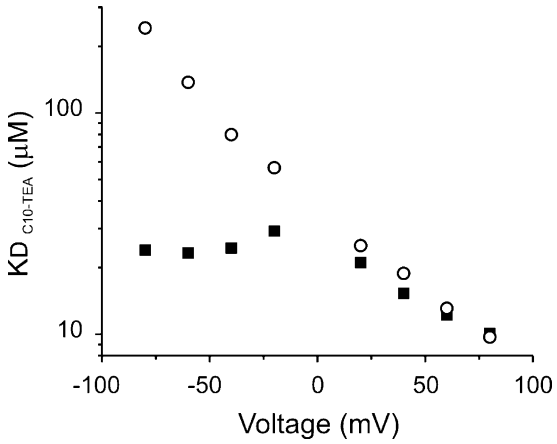

Figure 6. C10-TEA binds within the permeation pathway: the effect of external Mg^{2+} on intracellular C10-TEA blockade. Voltage dependence of intracellular C10-TEA blockade assessed in two different patches, either in the absence (open circles) or in the presence of 50 μM (filled squares) external Mg^{2+}.

and MacKinnon, 1993; Eismann et al., 1994; Park and MacKinnon, 1995; Gavazzo et al., 2000). Fig. 6 shows the voltage dependence of C10-TEA blockade in the absence (open circles) and in the presence of 50 μM (filled squares) extracellular Mg^{2+}. Strikingly, the presence of external Mg^{2+} altered the voltage dependence at negative potentials as if a reduction in ion permeation increases the apparent affinity of intracellular C10-TEA. These results support the idea that C10-TEA binds within the permeation pathway of open CNG channels.

State Dependence of QA Blockade: The Open State

To study open channel blockade we performed a series of experiments at the single channel level, assessing blockade under saturating concentrations of cGMP. Fig. 7 shows the activity at +70 mV of a single CNGA1 channel in the presence of 2 mM cGMP (Fig. 7 A) and after adding 5 μM C10-TEA to the intracellular side of the membrane (Fig. 7 B). Fig. 7 (C and D) shows the corresponding current histograms from 20-s recordings in each condition. In each case, the solid line represents a fit to a Gaussian function with two components. In the absence of the blocker, the amplitude and area for the conductive state are 2.21 pA and 95%, respectively. The main effect of the blocker in the current distribution is to increase the area of the nonconductive level from 5% to 26%.

Since these experiments were done using saturating concentrations of cGMP, we tentatively represent these conditions by a simple kinetic model.

$$C_{2cGMP} \underset{k_{-1}}{\overset{k_1}{\rightleftharpoons}} O \overset{\text{C10-TEA}}{\underset{k_{off}}{\rightleftharpoons}} OB \qquad \text{(SCHEME 1)}$$

In the absence of the blocker, the apparent open time constant is defined as $1/k_{-1}$. However, if C10-TEA binds to an open channel, the open time distribution in the presence of the blocker should be shorter as the apparent open time constant is now determined by $1/(k_{-1} + k_{on}[\text{C10-TEA}])$. Fig. 8 (A and B) illustrates the open dwell-time distributions in the absence and in the presence of 25 μM C10-TEA, respectively. The solid lines

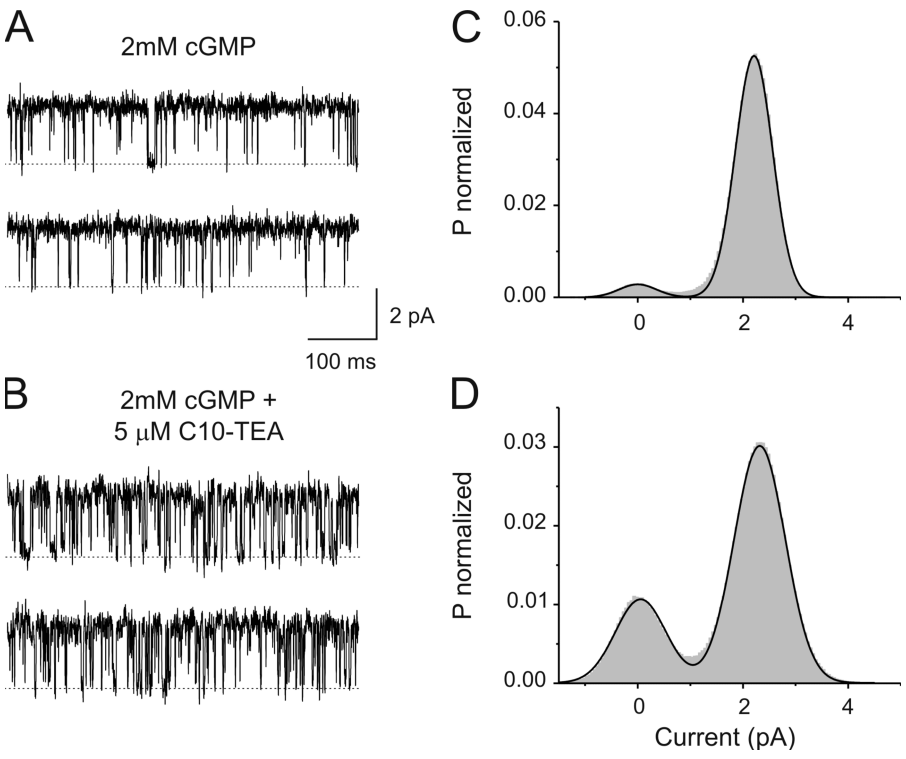

Figure 7. C10-TEA blockade at the single channel level. (A) Single channel recordings at +70 mV with solutions containing 2 mM cGMP. (B) Single channel recordings from the same channel in the presence of 2 mM cGMP and 5 μM of C10-TEA. Dashed lines represent the current level when the channel is closed. (C) Amplitude histogram from 20 s of recording in the presence of 2 mM cGMP. The solid line represents a two-component Gaussian fit. The best-fit parameter value for the amplitude for the open state was 2.209 ± 0.002 pA, comprising an area of 95%. (D) Amplitude histogram from 40 s of recording in the presence of 2 mM cGMP and 5 μM of C10-TEA. The solid line represents a two-component Gaussian fit. The best-fit parameter value for the amplitude for the open state was 2.317 ± 0.002 pA, contributing to an area of 74%.

represent double-exponential fits to the data. As predicted by an open channel blockade model, the presence of the blocker reduced the apparent mean open time of the main component from 12.2 to 3.74 ms. The minor fast component from these fits ($\tau \sim 0.7$ ms) remained unaltered by the presence of the blocker. Fig. 8 C shows the normalized dose response data obtained from four single-channel patches, all measured at +70 mV and in the presence of 2 mM cGMP. The solid line represents a Hill equation fit to the data. The best-fit parameter value for the midpoint was 16 ± 4 μM, which nicely matches our estimations of K_D using macroscopic currents under saturating cGMP concentrations.

State Dependence of QA Blockade: The Closed State

In CNG channels, the state occupancy can be manipulated by changing the concentration of the agonist. At saturating concentrations of cGMP, CNGA1 channels can achieve a maximal open probability (Po_{max}) of ≥0.95. At subsaturating concentrations of agonist, channels will tend to populate partially bound and unbound closed states (Ruiz and Karpen, 1997; Ruiz and Karpen, 1999). In the experiment shown in Fig. 9 A, we assessed blockade by 5 μM C10-TEA in saturating (left) and subsaturating (right) concentrations of cGMP. Blockade was larger at subsaturating levels of cGMP, suggesting that the blocker binds preferentially to closed channels. Alternatively, the state occupancy in CNGA1 channels can be altered by using saturating concentrations of agonists with different efficacies. For rod CNG channels, cGMP behaves as a full agonist while cIMP and cAMP are partial agonists, the latter being the least efficient (Varnum et al., 1995). Fig. 9 B shows three normalized pairs of leak-subtracted current traces in response to voltage steps to +80 mV under saturating agonist concentrations, and in the absence and presence of C10-TEA blocker, all obtained in the same inside-out patch. To be able to test these agonists in the same patch containing a fixed number of channels, we partially increased cAMP efficacy by adding 5 μM of Ni^{2+} to the internal solution (Gordon and Zagotta, 1995a). Blockade levels were larger for cIMP and cAMP, where the fully ligand-bound closed state has higher occupancy. These results are also consistent with blocker binding to closed channels. The simplest model to illustrate these new results is

(SCHEME 2)

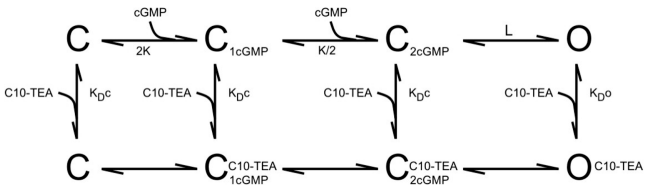

In this model, activation by cGMP is represented as two binding steps, a simplification that is sufficient to describe the macroscopic steady-state activation properties by cGMP (Karpen et al., 1988; Gordon and Zagotta, 1995b). K represents the equilibrium constant for cGMP binding to each subunit and L is the equilibrium constant of the allosteric transition from the closed

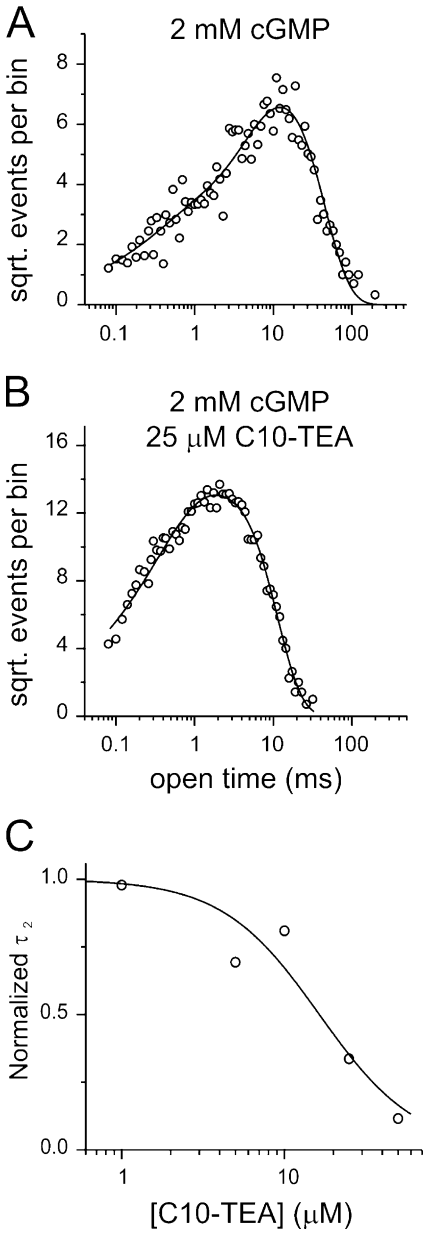

Figure 8. C10-TEA binds to an open channel. (A and B) Open dwell-time distributions at +70 mV under saturating (2 mM) cGMP concentrations in the absence and presence of 25 μM of C10-TEA. The solid lines represent double-exponential fits to the data. The best-fit parameter values were $\tau_1 = 0.7$ ms, $A_1 = 0.07$, $\tau_2 = 12.2$ ms, and $A_2 = 0.93$ in control conditions and $\tau_1 = 0.6$ ms, $A_1 = 0.19$, $\tau_2 = 3.7$ ms, and $A_2 = 0.81$ in the presence of the blocker. (C) C10-TEA dose response of the apparent mean open time of the slow component (τ_2). In each concentration, the effect of C10-TEA was normalized to the value of τ_2 in the absence of the blocker. The solid line represents a Hill equation fit with a best-fit parameter value for the midpoint of 16 ± 4 μM.

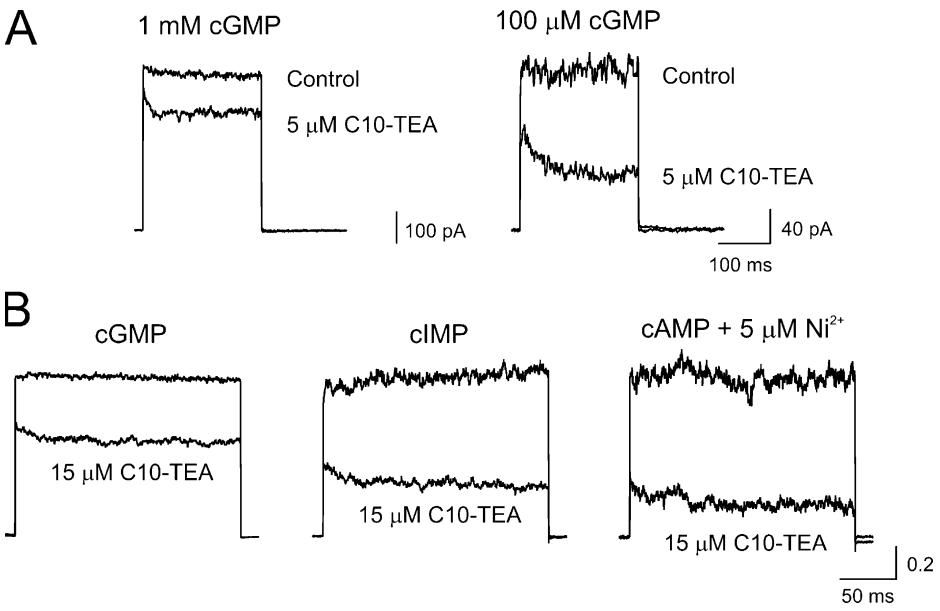

Figure 9. C10-TEA binds to closed channels: effects of agonists. (A) Leak-subtracted current traces to +80 mV in a patch where blockade by 5 μM C10-TEA was assessed under saturating (left) and subsaturating (right) concentrations of cGMP. (B) Leak-subtracted current traces to +80 mV in a patch where blockade by 15 μM C10-TEA was evaluated undersaturating (16mM) concentrations of cGMP (left), cIMP (middle), and cAMP (right). Each set of traces was normalized to a value of 1 in the absence of the blocker, therefore the ordinate scale lacks units.

to the open state. In addition, the model assumes that binding of C10-TEA in the closed states does not influence cGMP binding. A similar model has been used to describe blockade by tetracaine and dequalinium in CNG channels (Fodor et al., 1997b; Rosenbaum et al., 2004). We evaluated the effect of the blocker on the steady-state activation by cGMP. Fig. 10 shows the dose response at +70 mV for cGMP in the absence (open circles) and in the presence of 10 μM C10-TEA (filled circles). The solid line through the open circles represents a fit of Scheme 2 to the dose response data in the absence of the blocker. Because K and L are interdependent parameters, we fixed K to 3,500 M^{-1}, and allowed only L and the maximal current (I_{max}) to vary. The best-fit parameter value for L was 16 ± 2, which is similar to that previously found for CNGA1 channels expressed in oocytes (Fodor et al., 1997b), and for I_{max} was 2518 ± 39 pA. The solid line through the filled circles represents a fit of Scheme 2 to the dose response data in the presence 10 μM C10-TEA, with L and I_{max} fixed to the values estimated from the previous fit (i.e., in the absence of blocker). Therefore K_Dc and K_Do were the only two parameters permitted to vary. The best-fit parameter value for K_Do was 21 ± 2 μM, which is in good agreement with our previous estimations. The best-fit parameter value for K_Dc was 3 ± 0.2 μM. Using this strategy in four different patches gave an average K_Dc value of 2.3 ± 0.6 μM. Even though these results suggest a slightly higher apparent affinity of the blockers for the closed state, they do not address the kinetics of blockade, which, in principle, could influence the estimations of K_Dc. For example, imagine that at lower concentrations of cGMP, the blocker can only access its site while the channel is open, but upon channel closure in the blocker's presence, the closed state becomes stabilized. Under this scenario, the steady-state measurements might look relatively similar even though the blocker never reaches its site through a closed channel.

State-dependent Access of Triethylammonium-MTS reagents to the Inner Vestibule of CNG Channels

Direct determinations of ON and OFF rates for C10-TEA in the closed state are rather difficult. On the one hand, solution changes in inside-out patches are not fast enough to measure ON and OFF rates by traditional protocols relying on perfusion changes. On the other hand, the dwell-time distributions of shut time usually contains up to four exponential components in the absence of blocker (Holmgren, 2003), which would make it very challenging to elucidate new components in the presence of the blocker. Because of these difficulties, we used a chemical approach to gain some insights on whether the blocker accesses the inner vestibule of a closed CNG channel.

In Kv channels, the valine at the PVP consensus region has been shown, both structurally and functionally, to line the permeation pathway (Fig. 11 A). A cysteine mutation at this position revealed a large ($\sim 10^6\ M^{-1}s^{-1}$) state-dependent accessibility to MTSET reagent with modification rates as low as 1 $M^{-1}s^{-1}$ in the closed state (Liu et al., 1997). A cysteine substitution at the equivalent position in CNGA1 channels (Fig. 11 A) showed a much smaller difference between modification rates in the open and closed state (Flynn and Zagotta, 2001). In the same study, the state-dependent accessibility of MTSEA was shown to be minimal with modification rates in both closed and open state of ($\sim 10^3$–10^4 $M^{-1}s^{-1}$), comparable to modification rates in the open state by MTSET. The difference between these two

reagents is their sizes; MTSET is a quaternary amine (trimethylammonium ethyl-MTS) while MTSEA is a primary amine (amino ethyl-MTS). Since the blockers used in our study are triethylammonium derivatives, we asked if comparably sized MTS reagents (MTS-PtrEA and MTS-TEA) could access position 391C in the closed state and how these modification rates compare to those measured in the open state. Fig. 11 B illustrates the experimental protocols for open and closed state modification. MTS reagents were applied for 2 s in the absence (closed state) or presence of 2 mM cGMP (open state), and channel activity was monitored by a brief 50-ms pulse to +80 mV. Fig. 11 C shows two experiments in which modification by 500 μM MTS-PtrEA was assessed in the open (open circles) and in the closed state (filled circles) in cysteine-less CNGA1channels. Solid lines represent single exponential fits. The best-fit parameter values for the time constant (τ) were 5.7 ± 0.3 and 27 ± 1 s for the open and closed state, respectively. From these values we estimated a modification rate of 351 $M^{-1}s^{-1}$ for the open state and a rate of 74 $M^{-1}s^{-1}$ for the closed state. The average modification rates for open and closed states for both MTS-PtrEA and MTSTEA are shown in Fig. 11 D. For both reagents, the modification rates are about three to seven times faster in the open than in the closed state. In addition, we also show the modification rates for MTSET. Remarkably, the state dependence for the larger reagents is smaller than that for MTSET even though the modification rates for the closed state are comparable for all MTS reagents tested. These results show that there is not much impediment to access the inner vestibule of a closed CNG channel with molecules of similar structure as QA blockers and suggest that the ON rate of blockers in the closed state is at worst seven times slower than in an open channel.

C10-TEA Slows Chemical Modification at the Inner Vestibule of Closed CNG Channels

If QA blockers bind in the closed state, they might be able to inhibit the chemical modification of cysteine substituted at position 391. It would be rather difficult to interpret these experiments if we use MTS reagents. First, the MTS reagents tested are quaternary ammonium compounds, and we know that CNGA1 channels are blocked by essentially any quaternary ammonium derivatives, and second, the modification rates measured in the closed state are relatively slow. As an alternative, we used Cd^{2+} ions, which have been reported to interact with position 391 (Giorgetti et al., 2005). The experimental protocols (Fig. 12 A) are similar to those used for MTS modification. Cd^{2+} modifications were done in the complete absence of cGMP with solutions lacking divalent chelators. Immediately after the 2-s Cd^{2+} treatment, the patch was perfused for 2 s with a solution containing 200 μM EDTA to quickly chelate any remnant of Cd^{2+} ions. When modification was assessed

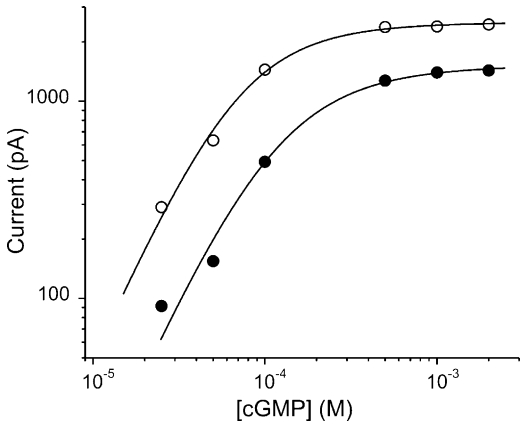

Figure 10. C10-TEA binds to closed channels: steady-state cGMP activation. Open circles show the dose response for cGMP in the absence of C10-TEA. The solid line represents a fit of Scheme 2 to the dose response data. Parameter K was fixed at 3500 M^{-1} (Fodor et al., 1997a), and L and Imax were allowed to vary. The best-fit parameter values for L and Imax were 16 ± 1 and 2533 ± 45 pA, respectively. Filled circles illustrate the dose response for cGMP in the presence of 10 μM C10-TEA. The solid line symbolizes a fit of the model shown in text to the dose response data. In this fit, L and I_{max} were fixed to the values obtained in the absence of the blocker. The best-fit parameter values for K_Dc and K_Do were 3 ± 0.3 and 21 ± 2 μM, respectively.

in the presence of C10-TEA, Cd^{2+} treatments were bracketed by 2 s of solutions containing C10-TEA in the absence of Cd^{2+} ions. Fig. 12 B (filled circles) shows that the current activated by cGMP is inhibited by successive exposures to 6 μM Cd^{2+} in the closed state. The interactions of Cd^{2+} ions are specific to 391C because even 50 μM Cd^{2+} has no effect on the cysteine-less wild-type channels (unpublished data). Cd^{2+} interactions with 391C in CNGA1 channels are not as strong as those observed with 474C Shaker Kv channels. In CNGA1 channel, the current inhibition does recover ∼20–40%, but with a very slow time course (τ ∼ 100 s; unpublished data). The presence of 200 μM C10-TEA in the complete absence of cGMP substantially slowed the current inhibition observed by Cd^{2+} ions (Fig. 12 B; filled squares). Since the channels were never opened by cGMP when they were exposed to C10-TEA and Cd^{2+} ions, these results show that the blocker was able to interfere with the access of Cd^{2+} ions to position 391C when the channels were closed, strongly suggesting that the blocker can bind in the closed state.

DISCUSSION

General Properties of QA Blockade in CNGA1 Channels

The object of the present study was to examine the interactions between QA derivatives and the intracellular pore of CNGA1 channels. At saturating [cGMP], QA compounds applied intracellularly blocked ion permeation

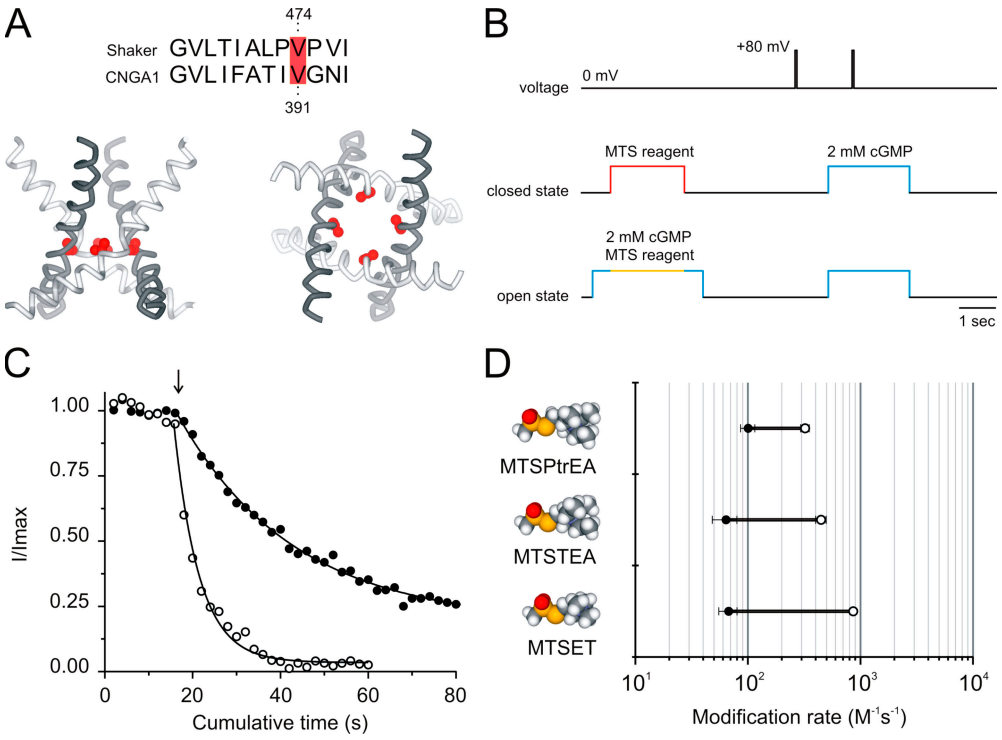

Figure 11. MTS reagents of comparable sizes to QA blockers can access position V391C in closed CNGA1 channels. (A) Alignment of the intracellular side of the S6 segment of Shaker Kv and CNGA1 channels. In red is highlighted the position where chemical modification was assessed. The bottom part shows the S6 helices from the X-ray crystal structure of Kv1.2 (Long et al., 2005). On the left is shown a side view of the S6 helices and on the right is shown an intracellular view. C^{β} and C^{γ} atoms of V474 are represented in red. (B) The experimental protocol consisted of 2-s reagent application at 0 mV in the presence (open state) or absence (closed state) of 2 mM cGMP. A brief 50-ms depolarization to +80 mV in the presence of 2 mM cGMP was applied to monitor the cGMP-activated current (blue step). Leak currents were acquired by a similar pulse to +80 mV but in the absence of cGMP. This protocol was applied every 15 s. (C) Modification of 391C CNGA1 channels by 500 μM MTS-PtrEA in the open (open circles) and in the closed states (filled circles). Circles symbolize leak-subtracted currents normalized to the average maximal current from the eight records acquired previous to MTS-PtrEA treatment (arrow). The decrease in cGMP-dependent currents were fitted to single exponentials (solid lines). The best-fitted parameter values for τ were 5.7 ± 0.3 and 27 ± 1 s for the open and closed state, respectively. (D) Modification rates in the open (open circles) and closed states (filled circles) for 391C CNGA1 channels by three different MTS reagents. Structural models of each reagent are shown. Symbols represent the mean of at least three experiments.

in a voltage-dependent manner ($z\delta \sim -0.4$) with properties that can be described by a simple model in which one molecule of QA interacts with one channel. In addition, the apparent affinity of the blockers strongly correlates with the hydrophobicity of each compound. The binding energy increased by 1.22 RT per methylene group added, similar to the energy needed to transfer a methylene group from a nonpolar medium to an aqueous solution (Tanford, 1980). These results suggest that somewhere within the intracellular mouth of a CNG channel there is a hydrophobic pocket that serves as part of the receptor for QA compounds. Finally, extracellular divalent ions greatly influenced the apparent affinity of blocker applied on the intracellular side, suggesting that QA derivatives bind within the permeation pathway of the channel. All these properties of QA blockade in CNGA1 channels are reminiscent of QA blockade of Kv channels (Armstrong, 1966, 1969, 1971; Armstrong and Hille, 1972; Choi et al., 1993), suggesting that these compounds might bind to a similar region of the intracellular mouth in these two types of channels. In potassium channels, where our understanding of the blockade mechanism is better developed, we now know that QA compounds bind to a hydrophobic pocket within the intracellular cavity of the channel (Choi et al., 1993; Zhou et al., 2001).

Previous blockade studies in CNG channels are also consistent with the presence of a hydrophobic pocket within the intracellular mouth of the channel. Using a series of tetraalkylammonium compounds, Stotz and Haynes (1996) showed that in both rod and cone CNG channels, the apparent affinities increased monotonically as the length of the alkyl chains increased. Similarly, by removing the hydrophobic end of tetracaine, the apparent affinity at 0 mV decreased by ~1,000-fold (Strassmaier et al., 2005). Since the receptor for these compounds likely shares some region with the receptor of the QA derivatives tested by us, it is reasonable to suggest that this hydrophobic pocket is located within the permeation pathway of CNG channels.

State Dependence of QA Blockade: Implications in Gating by cGMP

We have found that at positive potentials, QA blockers bind to CNGA1 channels in both open and closed states. In the open state, the apparent affinity for C10-TEA at +70 mV is ~20 μM, while in the closed state is ~2.5 μM. Since the apparent affinity of the closed state

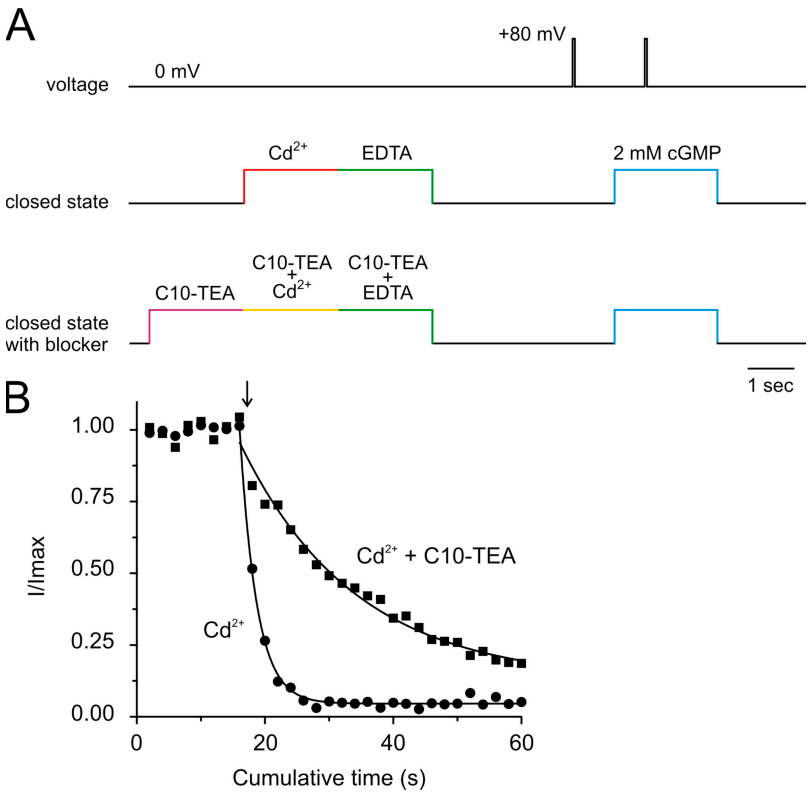

Figure 12. C10-TEA slows Cd^{2+} inhibition of 391C CNGA1 channels in the closed state. (A) The experimental protocol consisted of 2-s treatment with 6 μM Cd^{2+} ions with solutions lacking divalent chelators. Immediately after treatment, the patch was perfused with a solution containing 200 μM EDTA to quickly chelate any Cd^{2+} contamination. In addition, when the effect of the presence of C10-TEA was assessed, the Cd^{2+}-C10-TEA treatment was preceded and followed by 2-s perfusion with solutions containing C10-TEA in the absence of Cd^{2+}. (B) Filled circles correspond to an experiment in which 6 μM Cd^{2+} treatments in the closed state were initiated at the arrow. The solid line through symbols represents a single exponential fit. The best-fit parameter value for τ was 2.64 ± 0.08 s. Filled squares symbolize an experiment in which 6 μM Cd^{2+} was applied in the presence of 200 μM C10-TEA. In this case, the best-fit parameter value for τ was 18 ± 2 s.

was determined by steady-state measurements, it does not address whether the blocker can enter the blocking site when the channel is closed. Even though we do not have direct kinetic information on the blockade of closed channels, the chemical modification in the closed state of position 391C by MTS reagents of comparable sizes to the blockers and the ability of C10-TEA to slow the Cd^{2+} interactions with 391C suggest that the blockers can indeed access their binding sites while the channels are closed. The apparent preference of QA blockers for the closed state has also been observed for other blockers tested in CNGA1 channels. Tetracaine and some of its derivatives blocked CNGA1 channels with apparent affinities of almost 10^3 times higher in the closed state as compared with those estimated in the open state (Fodor et al., 1997b; Ghatpande et al., 2003). Similar to our observations, dequalinium has been shown to block closed CNGA1 channels with only three- to fivefold higher apparent affinities than open channels (Rosenbaum et al., 2004). We believe that QA blockade in the closed state is not a peculiarity of CNGA1 channels, because when we cotransfect rod α and β subunits, the only appreciable difference is a slight increase in apparent affinity with no changes in the state dependence of blockade (unpublished data).

QA blockade in Kv channels is tightly coupled to the state of the channel. QA compounds, when applied intracellularly, can bind only after the channel has been opened by depolarization (Armstrong, 1971; Choi et al., 1993). In addition, it was shown that the blocker can be trapped within the channel by closing the gate upon repolarization (Armstrong, 1971; Armstrong and Hille, 1972; Holmgren et al., 1997), suggesting that the gate that opens and closes the permeation pathway in response to voltage is located somewhere in the intracellular part of the protein. In stark contrast to Kv channels, our results do not support a similar gating mechanism for CNG channels. In CNG channels, QA compounds can bind to both open and closed states. Assuming that QA compounds bind in a similar site when CNGA1 channels are open or closed, the discrepancies between CNG and Kv channels suggest that these channels gate by different mechanisms.

In Kv channels, the gate that responds to voltage was found to be on the intracellular end of the last transmembrane segment. State-dependent reactivity of cysteine substitutions along this region showed a clear pattern in which residues located deeper than I477 were modified almost exclusively in the open state, while residues toward the COOH terminus were easily modified irrespectively of the state of the channel (Liu et al., 1997). In addition, large state-dependent modification was also found for Ag^+ ions, a cysteine modifier of comparable size to K^+ ions (del Camino and Yellen, 2001). When a similar approach was applied to CNG channels, it did not reveal the same pattern (Flynn and Zagotta, 2001). Residues situated deep in the pore showed some state dependence for larger cation reagents like MTSET, but

none for smaller modifiers like MTSEA and Ag^+ ions. These results, like our observations, are also consistent with the idea that the gate responsible for preventing permeation at high rates in the closed state of CNG channels is not at the intracellular end of the channel. Where is the gate that responds to cGMP? The answer to this question still remains elusive in CNG channels. Previous cysteine scanning mutagenesis studies along the P-region do not provide a clear pattern between intracellular and extracellular chemical accessibility (Sun et al., 1996; Becchetti et al., 1999; Becchetti and Roncaglia, 2000), although conformational changes associated with gating have been reported in both the S6 region (Flynn and Zagotta, 2001) and the P-region of CNG channels (Liu and Siegelbaum, 2000; Mazzolini et al., 2002). It will be interesting to further examine the location of the activation gate in CNG channels with experiments targeting the selectivity filter.

This work was possible thanks to Gary Yellen, who provided propyl-, butyl-, octyl-, and decyltriethyl ammonium, and MTSTEA. We would like to thank David Naranjo, Alan Neely, Shai Silberberg, Andrew Plested, Joe Mindell, and Kenton Swartz for helpful discussions. Finally, we thank Deepa Srikumar for a steady supply of HEK293 cells.

J.E. Contreras is supported by a Ruth L. Kirschstein postdoctoral fellowship. This research was supported by the Intramural Research Program of the National Institutes of Health, National Institute of Neurological Disorders and Stroke.

Olaf S. Andersen served as editor.

Submitted: 19 October 2005
Accepted: 21 March 2006

REFERENCES

Armstrong, C.M. 1966. Time course of TEA^+-induced anomalous rectification in squid giant axons. *J. Gen. Physiol.* 50:491–503.

Armstrong, C.M. 1969. Inactivation of the potassium conductance and related phenomena caused by quaternary ammonium ion injection in squid axons. *J. Gen. Physiol.* 54:553–575.

Armstrong, C.M. 1971. Interaction of tetraethylammonium ion derivatives with the potassium channels of giant axons. *J. Gen. Physiol.* 58:413–437.

Armstrong, C.M., and B. Hille. 1972. The inner quaternary ammonium ion receptor in potassium channels of the node of Ranvier. *J. Gen. Physiol.* 59:388–400.

Becchetti, A., K. Gamel, and V. Torre. 1999. Cyclic nucleotide-gated channels. Pore topology studied through the accessibility of reporter cysteines. *J. Gen. Physiol.* 114:377–392.

Becchetti, A., and P. Roncaglia. 2000. Cyclic nucleotide-gated channels: intra- and extracellular accessibility to Cd^{2+} of substituted cysteine residues within the P-loop. *Pflugers Arch.* 440:556–565.

Bonigk, W., W. Altenhofen, F. Muller, A. Dose, M. Illing, R.S. Molday, and U.B. Kaupp. 1993. Rod and cone photoreceptor cells express distinct genes for cGMP-gated channels. *Neuron.* 10:865–877.

Bonigk, W., J. Bradley, F. Muller, F. Sesti, I. Boekhoff, G.V. Ronnett, U.B. Kaupp, and S. Frings. 1999. The native rat olfactory cyclic nucleotide-gated channel is composed of three distinct subunits. *J. Neurosci.* 19:5332–5347.

Brown, R.L., T.L. Haley, K.A. West, and J.W. Crabb. 1999. Pseudechetoxin: a peptide blocker of cyclic nucleotide-gated ion channels. *Proc. Natl. Acad. Sci. USA.* 96:754–759.

Chen, T.Y., Y.W. Peng, R.S. Dhallan, B. Ahamed, R.R. Reed, and K.W. Yau. 1993. A new subunit of the cyclic nucleotide-gated cation channel in retinal rods. *Nature.* 362:764–767.

Choi, K.L., C. Mossman, J. Aube, and G. Yellen. 1993. The internal quaternary ammonium receptor site of Shaker potassium channels. *Neuron.* 10:533–541.

Colamartino, G., A. Menini, and V. Torre. 1991. Blockage and permeation of divalent cations through the cyclic GMP-activated channel from tiger salamander retinal rods. *J. Physiol.* 440:189–206.

Crary, J.I., D.M. Dean, W. Nguitragool, P.T. Kurshan, and A.L. Zimmerman. 2000. Mechanism of inhibition of cyclic nucleotide-gated ion channels by diacylglycerol. *J. Gen. Physiol.* 116:755–768.

Dean, D.M., W. Nguitragool, A. Miri, S.L. McCabe, and A.L. Zimmerman. 2002. All-trans-retinal shuts down rod cyclic nucleotide-gated ion channels: a novel role for photoreceptor retinoids in the response to bright light? *Proc. Natl. Acad. Sci. USA.* 99:8372–8377.

del Camino, D., M. Holmgren, Y. Liu, and G. Yellen. 2000. Blocker protection in the pore of a voltage-gated K^+ channel and its structural implications. *Nature.* 403:321–325.

del Camino, D., and G. Yellen. 2001. Tight steric closure at the intracellular activation gate of a voltage-gated K^+ channel. *Neuron.* 32:649–656.

Dhallan, R.S., K.W. Yau, K.A. Schrader, and R.R. Reed. 1990. Primary structure and functional expression of a cyclic nucleotide-activated channel from olfactory neurons. *Nature.* 347:184–187.

Eismann, E., F. Muller, S.H. Heinemann, and U.B. Kaupp. 1994. A single negative charge within the pore region of a cGMP-gated channel controls rectification, Ca^{2+} blockage, and ionic selectivity. *Proc. Natl. Acad. Sci. USA.* 91:1109–1113.

Flynn, G.E., and W.N. Zagotta. 2001. Conformational changes in S6 coupled to the opening of cyclic nucleotide-gated channels. *Neuron.* 30:689–698.

Fodor, A.A., K.D. Black, and W.N. Zagotta. 1997a. Tetracaine reports a conformational change in the pore of cyclic nucleotide-gated channels. *J. Gen. Physiol.* 110:591–600.

Fodor, A.A., S.E. Gordon, and W.N. Zagotta. 1997b. Mechanism of tetracaine block of cyclic nucleotide-gated channels. *J. Gen. Physiol.* 109:3–14.

Gadsby, D.C., R.F. Rakowski, and P. De Weer. 1993. Extracellular access to the Na,K pump: pathway similar to ion channel. *Science.* 260:100–103.

Gavazzo, P., C. Picco, E. Eismann, U.B. Kaupp, and A. Menini. 2000. A point mutation in the pore region alters gating, Ca^{2+} blockage, and permeation of olfactory cyclic nucleotide-gated channels. *J. Gen. Physiol.* 116:311–326.

Ghatpande, A.S., R. Uma, and J.W. Karpen. 2003. A multiply charged tetracaine derivative blocks cyclic nucleotide-gated channels at subnanomolar concentrations. *Biochemistry.* 42:265–270.

Giorgetti, A., A.V. Nair, P. Codega, V. Torre, and P. Carloni. 2005. Structural basis of gating of CNG channels. *FEBS Lett.* 579:1968–1972.

Gordon, S.E., and W.N. Zagotta. 1995a. A histidine residue associated with the gate of the cyclic nucleotide-activated channels in rod photoreceptors. *Neuron.* 14:177–183.

Gordon, S.E., and W.N. Zagotta. 1995b. Localization of regions affecting an allosteric transition in cyclic nucleotide-activated channels. *Neuron.* 14:857–864.

Hamill, O.P., A. Marty, E. Neher, B. Sakmann, and F.J. Sigworth. 1981. Improved patch-clamp techniques for high-resolution current recording from cells and cell-free membrane patches. *Pflugers Arch.* 391:85–100.

Haynes, L.W. 1992. Block of the cyclic GMP-gated channel of vertebrate rod and cone photoreceptors by l-cis-diltiazem. *J. Gen. Physiol.* 100:783–801.

Holmgren, M. 2003. Influence of permeant ions on gating in cyclic nucleotide-gated channels. *J. Gen. Physiol.* 121:61–72.

Holmgren, M., M.E. Jurman, and G. Yellen. 1996. N-type inactivation and the S4-S5 region of the Shaker K^+ channel. *J. Gen. Physiol.* 108:195–206.

Holmgren, M., P.L. Smith, and G. Yellen. 1997. Trapping of organic blockers by closing of voltage-dependent K^+ channels: evidence for a trap door mechanism of activation gating. *J. Gen. Physiol.* 109:527–535.

Horrigan, D.M., M.L. Tetreault, N. Tsomaia, C. Vasileiou, B. Borhan, D.F. Mierke, R.K. Crouch, and A.L. Zimmerman. 2005. Defining the retinoid binding site in the rod cyclic nucleotide-gated channel. *J. Gen. Physiol.* 126:453–460.

Jan, L.Y., and Y.N. Jan. 1990. A superfamily of ion channels. *Nature.* 345:672.

Karpen, J.W., A.L. Zimmerman, L. Stryer, and D.A. Baylor. 1988. Gating kinetics of the cyclic-GMP-activated channel of retinal rods: flash photolysis and voltage-jump studies. *Proc. Natl. Acad. Sci. USA.* 85:1287–1291.

Kaupp, U.B., T. Niidome, T. Tanabe, S. Terada, W. Bonigk, W. Stuhmer, N.J. Cook, K. Kangawa, H. Matsuo, T. Hirose, et al. 1989. Primary structure and functional expression from complementary DNA of the rod photoreceptor cyclic GMP-gated channel. *Nature.* 342:762–766.

Kaupp, U.B., and R. Seifert. 2002. Cyclic nucleotide-gated ion channels. *Physiol. Rev.* 82:769–824.

Kramer, R.H., E. Goulding, and S.A. Siegelbaum. 1994. Potassium channel inactivation peptide blocks cyclic nucleotide-gated channels by binding to the conserved pore domain. *Neuron.* 12:655–662.

Lagnado, L., and D. Baylor. 1992. Signal flow in visual transduction. *Neuron.* 8:995–1002.

Liu, D.T., G.R. Tibbs, and S.A. Siegelbaum. 1996. Subunit stoichiometry of cyclic nucleotide-gated channels and effects of subunit order on channel function. *Neuron.* 16:983–990.

Liu, J., and S.A. Siegelbaum. 2000. Change of pore helix conformational state upon opening of cyclic nucleotide-gated channels. *Neuron.* 28:899–909.

Liu, Y., M. Holmgren, M.E. Jurman, and G. Yellen. 1997. Gated access to the pore of a voltage-dependent K^+ channel. *Neuron.* 19:175–184.

Long, S.B., E.B. Campbell, and R. Mackinnon. 2005. Crystal structure of a mammalian voltage-dependent Shaker family K^+ channel. *Science.* 309:897–903.

Lu, Z., and L. Ding. 1999. Blockade of a retinal cGMP-gated channel by polyamines. *J. Gen. Physiol.* 113:35–43.

Lynch, J.W. 1999. Rectification of the olfactory cyclic nucleotide-gated channel by intracellular polyamines. *J. Membr. Biol.* 170:213–227.

Matulef, K., G.E. Flynn, and W.N. Zagotta. 1999. Molecular rearrangements in the ligand-binding domain of cyclic nucleotide-gated channels. *Neuron.* 24:443–452.

Mazzolini, M., M. Punta, and V. Torre. 2002. Movement of the C-helix during the gating of cyclic nucleotide-gated channels. *Biophys. J.* 83:3283–3295.

McLatchie, L.M., and H.R. Matthews. 1992. Voltage-dependent block by L-cis-diltiazem of the cyclic GMP-activated conductance of salamander rods. *Proc. Biol. Sci.* 247:113–119.

McLatchie, L.M., and H.R. Matthews. 1994. The effect of pH on the block by L-cis-diltiazem and amiloride of the cyclic GMP-activated conductance of salamander rods. *Proc. Biol. Sci.* 255:231–236.

Menini, A. 1995. Cyclic nucleotide-gated channels in visual and olfactory transduction. *Biophys. Chem.* 55:185–196.

Nasi, E., and M. del Pilar Gomez. 1999. Divalent cation interactions with light-dependent K channels. Kinetics of voltage-dependent block and requirement for an open pore. *J. Gen. Physiol.* 114:653–672.

Pages, F., M. Ildefonse, M. Ragno, S. Crouzy, and N. Bennett. 2000. Coexpression of α and β subunits of the rod cyclic GMP-gated channel restores native sensitivity to cyclic AMP: role of D604/N1201. *Biophys. J.* 78:1227–1239.

Park, C.S., and R. MacKinnon. 1995. Divalent cation selectivity in a cyclic nucleotide-gated ion channel. *Biochemistry.* 34:13328–13333.

Peng, C., E.D. Rich, and M.D. Varnum. 2004. Subunit configuration of heteromeric cone cyclic nucleotide-gated channels. *Neuron.* 42:401–410.

Picones, A., and J.I. Korenbrot. 1995. Permeability and interaction of Ca^{2+} with cGMP-gated ion channels differ in retinal rod and cone photoreceptors. *Biophys. J.* 69:120–127.

Quandt, F.N., G.D. Nicol, and P.P. Schnetkamp. 1991. Voltage-dependent gating and block of the cyclic-GMP-dependent current in bovine rod outer segments. *Neuroscience.* 42:629–638.

Root, M.J., and R. MacKinnon. 1993. Identification of an external divalent cation-binding site in the pore of a cGMP-activated channel. *Neuron.* 11:459–466.

Root, M.J., and R. MacKinnon. 1994. Two identical noninteracting sites in an ion channel revealed by proton transfer. *Science.* 265:1852–1856.

Rosenbaum, T., A. Gordon-Shaag, L.D. Islas, J. Cooper, M. Munari, and S.E. Gordon. 2004. State-dependent block of CNG channels by dequalinium. *J. Gen. Physiol.* 123:295–304.

Rosenbaum, T., L.D. Islas, A.E. Carlson, and S.E. Gordon. 2003. Dequalinium: a novel, high-affinity blocker of CNGA1 channels. *J. Gen. Physiol.* 121:37–47.

Ruiz, M., and J.W. Karpen. 1999. Opening mechanism of a cyclic nucleotide-gated channel based on analysis of single channels locked in each liganded state. *J. Gen. Physiol.* 113:873–895.

Ruiz, M.L., and J.W. Karpen. 1997. Single cyclic nucleotide-gated channels locked in different ligand-bound states. *Nature.* 389:389–392.

Seifert, R., E. Eismann, J. Ludwig, A. Baumann, and U.B. Kaupp. 1999. Molecular determinants of a Ca^{2+}-binding site in the pore of cyclic nucleotide-gated channels: S5/S6 segments control affinity of intrapore glutamates. *EMBO J.* 18:119–130.

Spassova, M., and Z. Lu. 1999. Tuning the voltage dependence of tetraethylammonium block with permeant ions in an inward-rectifier K^+ channel. *J. Gen. Physiol.* 114:415–426.

Stotz, S.C., and L.W. Haynes. 1996. Block of the cGMP-gated cation channel of catfish rod and cone photoreceptors by organic cations. *Biophys. J.* 71:3136–3147.

Strassmaier, T., R. Uma, A.S. Ghatpande, T. Bandyopadhyay, M. Schaffer, J. Witte, P.G. McDougal, R.L. Brown, and J.W. Karpen. 2005. Modifications to the tetracaine scaffold produce cyclic nucleotide-gated channel blockers with widely varying efficacies. *J. Med. Chem.* 48:5805–5812.

Stryer, L. 1986. Cyclic GMP cascade of vision. *Annu. Rev. Neurosci.* 9:87–119.

Stryer, L. 1988. Molecular basis of visual excitation. *Cold Spring Harb. Symp. Quant. Biol.* 53:283–294.

Sun, Z.P., M.H. Akabas, E.H. Goulding, A. Karlin, and S.A. Siegelbaum. 1996. Exposure of residues in the cyclic nucleotide-gated channel pore: P region structure and function in gating. *Neuron.* 16:141–149.

Tanaka, J.C., and R.E. Furman. 1993. Divalent effects on cGMP-activated currents in excised patches from amphibian photoreceptors. *J. Membr. Biol.* 131:245–256.

Tanford, C. 1980. The Hydrophobic Effect: Formation of Micelles and Biological Membranes. Second edition. John Wiley and Sons, New York. 234 pp.

Varnum, M.D., K.D. Black, and W.N. Zagotta. 1995. Molecular mechanism for ligand discrimination of cyclic nucleotide-gated channels. *Neuron.* 15:619–625.

Weitz, D., N. Ficek, E. Kremmer, P.J. Bauer, and U.B. Kaupp. 2002. Subunit stoichiometry of the CNG channel of rod photoreceptors. *Neuron.* 36:881–889.

Woodhull, A.M. 1973. Ionic blockage of sodium channels in nerve. *J. Gen. Physiol.* 61:687–708.

Yau, K.W., and D.A. Baylor. 1989. Cyclic GMP-activated conductance of retinal photoreceptor cells. *Annu. Rev. Neurosci.* 12:289–327.

Zheng, J., M.C. Trudeau, and W.N. Zagotta. 2002. Rod cyclic nucleotide-gated channels have a stoichiometry of three CNGA1 subunits and one CNGB1 subunit. *Neuron.* 36:891–896.

Zheng, J., and W.N. Zagotta. 2004. Stoichiometry and assembly of olfactory cyclic nucleotide-gated channels. *Neuron.* 42:411–421.

Zhong, H., L.L. Molday, R.S. Molday, and K.W. Yau. 2002. The heteromeric cyclic nucleotide-gated channel adopts a 3A:1B stoichiometry. *Nature.* 420:193–198.

Zhou, M., J.H. Morais-Cabral, S. Mann, and R. MacKinnon. 2001. Potassium channel receptor site for the inactivation gate and quaternary amine inhibitors. *Nature.* 411:657–661.

Zimmerman, A.L. 1995. Cyclic nucleotide gated channels. *Curr. Opin. Neurobiol.* 5:296–303.

Zimmerman, A.L., and D.A. Baylor. 1992. Cation interactions within the cyclic GMP-activated channel of retinal rods from the tiger salamander. *J. Physiol.* 449:759–783.

Zufall, F., and S. Firestein. 1993. Divalent cations block the cyclic nucleotide-gated channel of olfactory receptor neurons. *J. Neurophysiol.* 69:1758–1768.

Zufall, F., S. Firestein, and G.M. Shepherd. 1994. Cyclic nucleotide-gated ion channels and sensory transduction in olfactory receptor neurons. *Annu. Rev. Biophys. Biomol. Struct.* 23:577–607.